Eur. J. Mineral.
2018, **30**, 537–544
Published online 10 January 2018

Ferriperbøeite-(Ce), $[CaCe_3]_{\sum=4}[Fe^{3+}Al_2Fe^{2+}]_{\sum=4}[Si_2O_7][SiO_4]_3O(OH)_2$, a new member of the polysomatic epidote–törnebohmite series from the Nya Bastnäs Fe-Cu-REE deposit, Sweden

LUCA BINDI[1,2,*], DAN HOLTSTAM[3], GIULIA FANTAPPIÈ[1], ULF B. ANDERSSON[4] and PAOLA BONAZZI[1]

[1] Dipartimento di Science de la Terra, Università degli Studi di Firenze, via G. La Pira 4, 50121 Firenze, Italy
*Corresponding author, e-mail: luca.bindi@unifi.it
[2] CNR – Istituto di Geoscienze e Georisorse, Sezione di Firenze, via G. La Pira 4, 50121 Firenze, Italy
[3] Department of Geosciences, Swedish Museum of Natural History, Box 50007, 104 05 Stockholm, Sweden
[4] Luossavaara-Kiirunavaara AB, R&D, TG, 981 86 Kiruna, Sweden

Abstract: Ferriperbøeite-(Ce), ideally $[CaCe_3]_{\sum=4}[Fe^{3+}Al_2Fe^{2+}]_{\sum=4}[Si_2O_7][SiO_4]_3O(OH)_2$, is a new mineral species from the Nya Bastnäs Fe–Cu–REE skarn deposit in the Bergslagen mining region (south-central Sweden). The mineral occurs in direct contact with ferriallanite-(Ce), cerite-(Ce) and törnebohmite-(Ce). In the type specimen, ferriperbøeite-(Ce) forms brownish black crystals, and exhibits an irregular to short-prismatic morphology elongated along [0 1 0]. The maximum crystal size is about 500 μm. The mineral is optically biaxial positive, with $2V = 65 \pm 5°$. It is strongly pleochroic from green, throughout orange-brown, to deep red colours. Electron microprobe analyses yields the empirical formula, calculated on the basis of 13 cations and divalent and trivalent iron partitioned to fulfill the criterion of charge balance, $(Ca_{0.92}La_{1.23}Ce_{1.50}Pr_{0.10}Nd_{0.27}Sm_{0.02}Y_{0.01})_{\sum=4.05}(Al_{1.85}Fe^{2+}_{0.46}Fe^{3+}_{1.13}Mg_{0.57}Ti_{0.01})_{\sum=4.02}(Si_{4.92}P_{0.01})_{\sum=4.93}O_{20}(OH_{1.87}F_{0.12}Cl_{0.01})$, which is in accord with single-crystal X-ray diffraction, infra-red, and Mössbauer spectroscopy data. The mineral is monoclinic, space group $P2_1/m$, with unit-cell parameters: $a = 8.9320(4)$, $b = 5.7280(3)$, $c = 17.5549(9)$ Å, $\beta = 116.030(4)°$, $V = 807.05(7)$ Å^3, $Z = 2$. Ferriperbøeite-(Ce) is as a new member of the epidote (E) – törnebohmite (T) polysomatic series, having an E module with ferriallanite-(Ce) composition. The new mineral and the mineral name have been approved by the Commission on New Minerals, Nomenclature and Classification, IMA 2017-037.

Key-words: ferriperbøeite-(Ce); new mineral species; epidote; törnebohmite-(Ce); electron-microprobe analyses; Mössbauer spectrum; infra-red spectrum; crystal structure; polysome; Bastnäs-type deposits; Sweden.

1. Introduction

Minerals belonging to the gatelite supergroup (Bonazzi *et al.*, 2017) can be regarded as iso-topological ET polysomes of a series having epidote and törnebohmite-(Ce) as end-members. They include gatelite-(Ce) (Bonazzi *et al.*, 2003), västmanlandite-(Ce) (Holtstam *et al.*, 2005), perbøeite-(Ce) and alnaperbøeite-(Ce) (Bonazzi *et al.*, 2014). While the T module exhibits an almost invariable composition, the variable composition of the E module differentiates each member. In particular, the E module exhibits a dissakisite-(Ce) composition in gatelite-(Ce), dollaseite-(Ce) composition in västmanlandite-(Ce), and allanite-(Ce) composition in perbøeite-(Ce), whereas for alnaperbøeite-(Ce) the E module corresponds to a new, Na-bearing REE-epidote composition $[(Ca,REE,Na)Al_3(Si_2O_7)(SiO_4)O(OH)]$. However, minerals having an E module corresponding to a ferriallanite-(Ce) (Kartashov *et al.*, 2002) composition have also been reported: the Fe–O analogue of västmanlandite-(Ce) without F (labelled as UM2007-35 in the list of unnamed minerals; Smith & Nickel, 2007) from the Bergslagen region (Sweden) was noted by Holtstam & Andersson (2007), and a similar mineral is reported from carbonatite veins in Eastern Siberia, Russia (Gurzhiy *et al.*, 2010) and from a metamorphosed carbonatite sill in British Columbia, Canada (Ya'acoby, 2011).

The present paper reports the results of a chemical, structural and spectroscopic study of the sample #52:414, preliminary analysed by Holtstam & Andersson (2007), leading to the definition and description of a new member of the supergroup. By analogy with the IMA-approved nomenclature for the epidote supergroup minerals, and to underline the substitutional relationships with perbøeite-(Ce), the mineral was named ferriperbøeite-(Ce). The mineral and the mineral name have been approved by IMA-CNMNC (2017–037). The holotype material, including a polished thin section, is deposited at the Swedish Museum of Natural History, Department of Geosciences, Box 50007, SE-10405 Stockholm, Sweden, under collection number NRM #52:414=#18520414.

https://doi.org/10.1127/ejm/2018/0030-2717
0935-1221/18/0030-2717 $ 3.60

2. Occurrence and paragenesis

The Bastnäs-type Fe–REE skarn deposits in the Bergslagen mining region (south-central Sweden) formed 1.90–1.84 Ga ago through reactions between pre-existing dolomitic carbonate layers and essentially juvenile magmatic (≥400 °C), saline fluids carrying Si, F, Cl, CO_2, in addition to REE and other metals (Holtstam *et al.*, 2014).

On the basis of the composition of the REE mineral assemblages, the deposits can be divided into two subtypes (Holtstam & Andersson, 2007): one almost exclusively with LREE enrichment (subtype 1, mainly in the Riddarhyttan–Bastnäs area), and another showing enrichment of both LREE and Y + HREE (subtype 2, Norberg District). REE silicates in subtype-1 deposits are Fe-rich, whereas those from subtype-2 deposits are high in Mg and F, which has governed the development of characteristic assemblages. This dichotomy is believed to reflect both real differences in fluid composition and variations in fluid/rock volumes (carbonate remnants are sparse at the subtype-1 deposits; Holtstam *et al.*, 2014).

Ferriperbøeite-(Ce), forming a solid solution series with västmanlandite-(Ce), was found in the subtype-1 deposits (Holtstam *et al.*, 2005; Holtstam & Andersson, 2007; Jonsson & Högdahl, 2013). The Fe-rich members of this series typically occur in direct contact with ferriallanite-(Ce) and are commonly closely associated with cerite-(Ce) and törnebohmite-(Ce).

The rock sample studied here (Fig. 1), from the Nya Bastnäs deposit, Skinnskatteberg, Västmanland (lat. 59°50′47″N, long. 15°35′15″E), was probably collected in the first half of the 19th century. It once belonged to the collection of Nils Wilhelm Almroth (1797–1852), a chemist and director of the Swedish Royal Mint, and was acquired by the Swedish Museum of Natural History after his death. Ferriperbøeite-(Ce) has developed as a major phase with crystal aggregates largely replacing cerite-(Ce); ferriallanite-(Ce) in turn occurs as a subordinate product of alteration, as crack-fillings and narrow rims on ferriperbøeite-(Ce). The dominating minerals in the type specimen are ferriperbøeite-(Ce), cerite-(Ce), törnebohmite-(Ce) and ferriallanite-(Ce) (Fig. 1, lower part). Törnebohmite-(Ce) occurs as inclusions in ferriperbøeite-(Ce), sometimes in the form of regular lamellae, and also as separate crystal aggregates in the cerite-(Ce)–ferriperbøeite-(Ce) mass. Minor constituents are bastnäsite-(Ce), chalcopyrite and bismuthinite. Late-stage Cu and Fe minerals, including brochantite and goethite, occur in cracks and on the surface of the specimen. A powdery, yellowish substance in association with grains of bastnäsite-(Ce) is tentatively identified as "håleniusite-(Ce)".

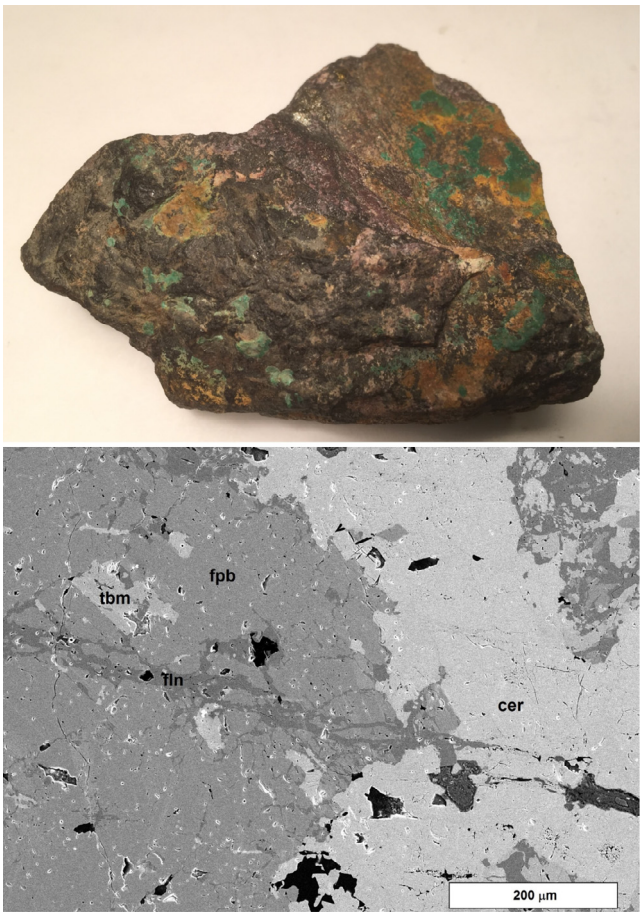

Fig. 1. Top: General view (incident light image) of the type specimen of ferriperbøeite-(Ce), #52:414 deposited at the Swedish Museum of Natural History. Size *ca.* 7.5 × 6 × 4 cm. Bottom: Field-emission SEM image of a polished section with ferriperbøeite-(Ce) (fpb) associated with törnebohmite-(Ce) (tbm), ferriallanite-(Ce) (fln), and cerite-(Ce) (cer). The darkest portions represent voids.

3. Appearance and physical properties

Ferriperbøeite-(Ce) is brownish black in colour and exhibits a subhedral to short-prismatic morphology; the crystals are elongated along [0 1 0] and twinning is not observed. The maximum crystal size is about 500 μm. The streak is brown and the lustre is vitreous; the crystals are transparent only in thin fragments, <20 μm. Ferriperbøeite-(Ce) is non-fluorescent. The mineral is relatively hard, likely corresponding to a Mohs hardness of 6–7. It is brittle and exhibits good {1 0 0} and imperfect {0 0 1} cleavage. The density could not be measured because of the small grain size and the presence of other minerals in the crystal aggregates. The calculated values are 4.610 g/cm^3, using the ideal formula and unit-cell parameters from X-ray single-crystal data, and 4.634 g/cm^3, using the empirical formula and unit-cell parameters from powder X-ray diffraction data.

The optical quality of the ferriperbøeite-(Ce) crystals is not optimal due to high absorption and numerous solid and fluid inclusions. Refractive indices could not be measured accurately for this reason. The mean refractive index was calculated according to the Gladstone-Dale relationship (Mandarino, 1981), $n_{calc} = 1.84$. The mineral is optically biaxial positive, with $2V = 65 \pm 5°$. It is strongly pleochroic, from green throughout orange-brown, to deep red colours.

To verify the presence of the ferriperbøeite-(Ce)–törnebohmite-(Ce) intergrowths in the crystal fragments of ferriperbøeite-(Ce) indicated by X-ray single-crystal

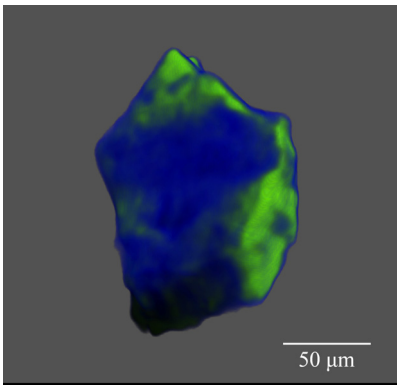

Fig. 2. MicroCT-scan image of a crystal of ferriperbøeite-(Ce) (blue) intergrown with törnebohmite-(Ce) (green).

diffraction experiments, one of them was studied by X-ray computed tomography (micro-CT scan). The instrument was a micro-CT SkyScan 1172 equipped with a 11Mpixel detector with a resolution of 0.8 mm and operating at 80 kV (X-ray tungsten radiation) with a spot size of 0.3 mm. The micro-CT scan study confirmed this result and showed that ferriperbøeite-(Ce) is indeed characterized by inclusions of törnebohmite-(Ce) (green in Fig. 2).

4. Chemical composition

Analyses were carried out using a Cameca SX50 electron microprobe (WDS mode, 20 kV, 40 nA and 3 μm beam diameter). The analytical results (mean results of 2 point analyses) are given in Table 1, together with the natural and synthetic standards used. Elements sought but not detected (0.01–0.05 wt% as detection limit) are Na, K, Sr, Ba, Mn, Th and U.

The empirical formula, calculated on the basis of 13 cations (except H) and partitioning divalent and trivalent iron to fulfil the criterion of charge balance, is: $(Ca_{0.92}La_{1.23}Ce_{1.50}Pr_{0.10}Nd_{0.27}Sm_{0.02}Y_{0.01})_{\Sigma=4.05}(Al_{1.85}Fe^{2+}_{0.46}Fe^{3+}_{1.13}Mg_{0.57}Ti_{0.01})_{\Sigma=4.02}(Si_{4.92}P_{0.01})_{\Sigma=4.93}O_{20}(OH_{1.87}F_{0.12}Cl_{0.01})$. The ideal formula, which takes into account results from Mössbauer and infra-red data and the single-crystal X-ray diffraction experiment, is $[CaCe_3]_{\Sigma=4}[Fe^{3+}Al_2Fe^{2+}]_{\Sigma=4}[Si_2O_7][SiO_4]_3O(OH)_2$. It requires: CaO 5.01, Ce_2O_3 43.93, Fe_2O_3 7.13, Al_2O_3 9.11, FeO 6.41, SiO_2 26.80, H_2O 1.61, total 100.00 wt%.

5. Infra-red and Mössbauer spectroscopy

Fourier transform infra-red (FTIR) spectroscopy was used to collect polarised single crystal spectra (Fig. 3) in the range 2000–5000 cm^{-1} from a 40 × 40 μm area of an unoriented crystal in a thin section of 30 μm thickness. The instrument was a Bruker Vertex 70 spectrometer attached to a Bruker Hyperion 2000 IR-microscope and measurements were done in 64 cycles at extinction positions (90°) of the grain, at a spectral resolution of 4 cm^{-1}.

A transmission ^{57}Fe Mössbauer spectrum (Fig. 4) was obtained from a 5 mg-powder absorber of ferriperbøeite-(Ce), using a ^{57}Co γ-radiation source (nominally 1.8 GBq). Two-mirror image spectra (±4.28 mm/s) were collected at 54.7° geometry during 400 h over 1024 channels and calibrated against an iron foil. Spectrum analysis was done assuming Lorentzian line shapes with the *MossA* program (Prescher *et al.*, 2012).

Table 1. Electron microprobe data and probe standards for ferriperbøeite-(Ce).

	wt%	Range	Probe standard
CaO	4.53	4.53–4.53	wollastonite
La_2O_3	17.62	17.51–17.73	synthetic $LaPO_4$
Ce_2O_3	21.57	21.47–21.67	synthetic $CePO_4$
Pr_2O_3	1.52	1.51–1.52	synthetic $PrPO_4$
Nd_2O_3	4.08	4.03–4.13	synthetic $NdPO_4$
Sm_2O_3	0.28	0.25–0.30	synthetic $SmPO_4$
Gd_2O_3	0.07	0.06–0.07	synthetic $GdPO_4$
Dy_2O_3	0.02	0.00–0.04	synthetic $DyPO_4$
Ho_2O_3	0.06	0.00–0.12	synthetic $HoPO_4$
Er_2O_3	0.00	0.00–0.00	synthetic $ErPO_4$
Yb_2O_3	0.01	0.00–0.02	synthetic $YbPO_4$
Lu_2O_3	0.02	0.00–0.03	synthetic $LuPO_4$
Y_2O_3	0.06	0.06–0.06	synthetic YPO_4
MgO	2.03	1.97–2.08	synthetic MgO
FeO	2.89	2.60–3.18	synthetic Fe_2O_3
Fe_2O_3*	7.92	7.49–8.34	
Al_2O_3	8.27	8.26–8.28	synthetic Al_2O_3
SiO_2	25.96	25.67–26.25	wollastonite
TiO_2	0.05	0.03–0.07	synthetic $MnTiO_3$
P_2O_5	0.08	0.06–0.09	fluorapatite
F	0.21	0.20–0.21	synthetic LiF
Cl	0.02	0.02–0.02	tugtupite
O=F	−0.09	−0.09–−0.08	
O=Cl	0.00	0.00–0.00	
Total	97.18	96.81–97.27	
H_2O§	1.50		
Total	98.68		

* Fe^{2+}/Fe^{3+} calculated to obtain charge neutrality
§ H_2O calculated on the basis of OH = 1.87 pfu.

6. X-ray crystallography

A small ferriperbøeite-(Ce) crystal fragment (50 × 55 × 65 $μm^3$) was extracted from the available sample under a stereomicroscope and mounted on a 5 μm diameter carbon fibre, which was, in turn, attached to a glass rod. Single-crystal X-ray diffraction intensity data were collected using an Oxford Diffraction Xcalibur diffractometer equipped with an Oxford Diffraction CCD detector, with graphite-monochromatised Mo*K*α radiation (λ = 0.71073 Å). The data were integrated and corrected for standard Lorentz and polarization factors with the *CrysAlis* RED package (Oxford Diffraction, 2006). The program ABSPACK in *CrysAlis* RED (Oxford Diffraction, 2006) was used for the absorption correction. A total of 3454 unique reflections was collected.

No evidence of the doubling of the translation unit along the **a**-axis observed in gatelite-(Ce) was found in ferriperbøeite-(Ce). Thus, the structure was refined in

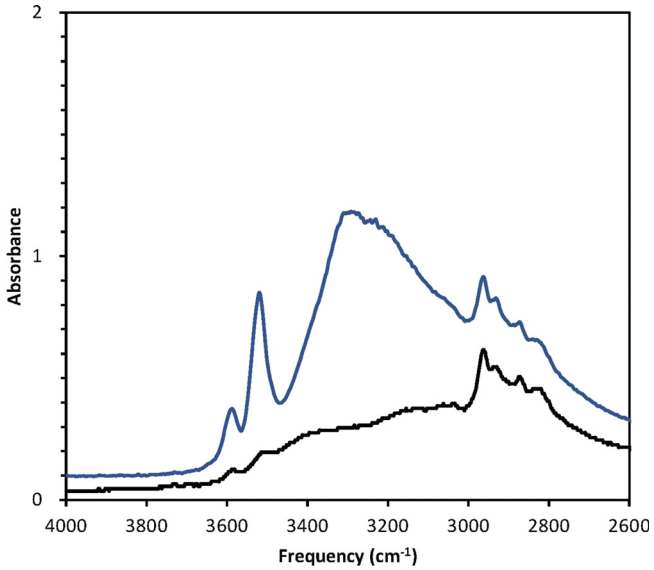

Fig. 3. Polarised FTIR spectra of ferriperbøeite-(Ce) measured at two perpendicular extinction positions (blue and black curves) on a grain of unspecified orientation. The band features at 2800–3000 cm^{-1} are related to C–H stretching in the thin (~2 μm) layer of epoxy resin between sample and glass holder.

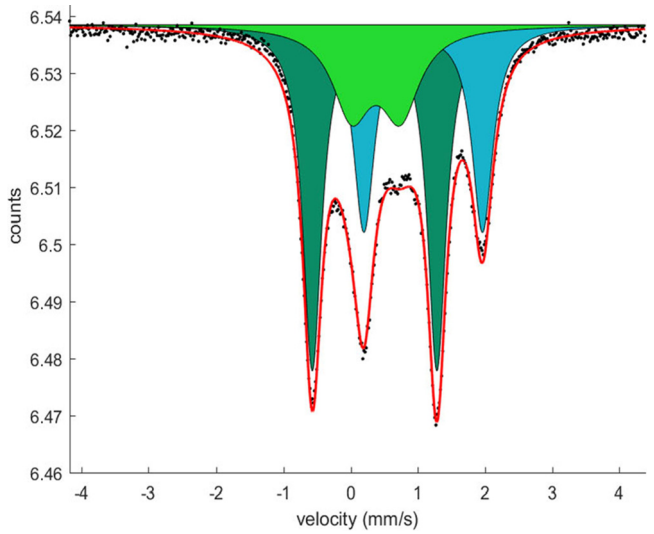

Fig. 4. Transmission ^{57}Fe spectrum of ferriperbøeite-(Ce). Dark and light green doublets correspond to the fitted A and C Fe^{3+}-subspectra, respectively. The light blue doublet is the B $^{M3}Fe^{2+}$ subspectrum (see Table 7).

the $P2_1/m$ instead of $P2_1/a$ space group starting from the atomic coordinates reported for perbøeite-(Ce) (Bonazzi *et al.*, 2014), using the program *SHELXL2013* (Sheldrick, 2013). The site occupation factor at the cation sites was allowed to vary (Ca *vs.* Ce for the A sites; Fe *vs.* Mg for M1 and M3 and Al *vs.* Fe for M2) using scattering curves for neutral atoms taken from the International Tables for Crystallography (Wilson, 1992). No hydrogen atoms were located on the ΔF map. The refinement converged to $R_1 = 0.0460$ for 2530 reflections with $F_o > 4\sigma(F_o)$ and 0.0745 for all 3454 independent reflections and 203 parameters. Experimental details of the refinement are given in Table 2. Final atomic coordinates and equivalent isotropic displacement parameters are presented in Table 3, anisotropic displacement parameters in Table 4 (deposited), whereas bond distances and angles are shown in Table 5. The CIF of the ferriperbøeite-(Ce) structure, which includes the list of observed and calculated structure factors, is available as supplementary material on the GSW site of the journal https://pubs.geoscienceworld.org/eurjmin.

Table 2. Crystal data and summary of parameters describing data collection and refinement for ferriperbøeite-(Ce).

Crystal data	
Ideal formula	$[CaCe_3]_{\Sigma=4}[Fe^{3+}Al_2Fe^{2+}]_{\Sigma=4}[Si_2O_7][SiO_4]_3O(OH)_2$
Crystal size (mm^3)	0.050 × 0.055 × 0.065
Cell setting, space group	Monoclinic, $P2_1/m$
a, *b*, *c* (Å)	8.9320(4), 5.7280(3), 17.5549(9)
α, β, γ (°)	90, 116.030(4), 90
V ($Å^3$)	807.05(7)
Z	2
Data collection and refinement	
Radiation, wavelength (Å)	Mo*K*α, λ = 0.71073
Temperature (K)	293
Maximum observed 2θ (°)	69.14
Measured reflections	11005
Unique reflections	3454
Reflections $F_o > 4\sigma(F_o)$	2530
R_{int} after absorption correction	0.0609
$R\sigma$	0.0727
Range of *h*, *k*, *l*	$-13 \le h \le 13$, $-8 \le k \le 8$, $-26 \le l \le 27$
R [$F_o > 4\ \sigma\ F_o$]	0.0460
R (all data)	0.0745
wR (on F_o^2)	0.0952
Goof	1.046
No. of least-squares parameters	203
Max. and min. residual peak ($e/Å^3$)	2.44; −3.29

A powder X-ray diffraction pattern was recorded with step (0.02°) scans in the 2θ-range 3 to 65° on an automated Philips PW1710 diffractometer using graphite-monochromatised Cu*K*α radiation (PW1830 generator operated at 40 kV and 40 mA). Peak positions were determined with the X'Pert Graphics & Identify program and corrected against an external silicon standard (NBS 640b). Indexed *d* values for reflections with $2\theta \le 50°$ and relative peak heights above background are given in Table 6. The monoclinic unit-cell parameters, obtained by least-squares refinement of 40 reflections, are $a = 8.9317(5)$ Å, $b = 5.7441(4)$ Å, $c = 17.6164(9)$ Å, $\beta = 116.034(4)°$ and $V = 812.09(5)$ $Å^3$.

7. Discussion

7.1. Description of the structure

The crystal structure of ferriperbøeite-(Ce) is shown in Fig. 5. It consists of edge-sharing octahedral chains running along the **b**-axis, cross-linked to each other by SiO_4 and Si_2O_7 groups. The remaining large cavities are

Table 3. Site occupancy factors (s.o.f.), atom coordinates and equivalent isotropic displacement parameters (in Å^2) in ferriperbøeite-(Ce).

Atom	s.o.f.	*x*	*y*	*z*	U^{iso}
A1	$Ca_{0.954(4)}Ce_{0.046}$	0.7277(2)	¼	0.4088(1)	0.0142(5)
A2	Ce	0.89030(6)	¼	0.24925(3)	0.0127(1)
A3	Ce	0.73786(7)	¼	0.00916(3)	0.0256(2)
A4	Ce	0.07573(6)	¾	0.16526(3)	0.0117(1)
M1	$Fe_{0.658(9)}Mg_{0.342}$	½	½	½	0.0081(4)
M2	$Al_{0.937(7)}Fe_{0.063}$	0.4789(2)	0.0000(3)	0.2042(1)	0.0083(5)
M3	$Fe_{0.790(9)}Mg_{0.210}$	0.1910(2)	¾	0.37575(9)	0.0122(4)
Si1	Si	0.1550(3)	¼	0.4775(1)	0.0088(4)
Si2	Si	0.8023(3)	¾	0.3342(1)	0.0082(4)
Si3	Si	0.3012(3)	¼	0.3109(1)	0.0060(4)
Si4	Si	0.6688(3)	¾	0.1028(1)	0.0098(4)
Si5	Si	0.1537(3)	¼	0.0773(1)	0.0084(4)
O1	O	0.2581(5)	0.4911(7)	0.4815(3)	0.0126(8)
O2	O	0.1766(5)	0.4723(8)	0.2895(3)	0.0135(8)
O3	O	0.6913(5)	0.9849(8)	0.2991(3)	0.0137(8)
O4	O	0.4382(7)	¾	0.4193(4)	0.010(1)
O5	O	0.4495(7)	¼	0.4102(4)	0.010(1)
O6	O	0.4130(7)	¼	0.2570(4)	0.011(1)
O7	O	−0.0219(7)	¼	0.3986(4)	0.014(1)
O8	O	−0.0493(7)	¾	0.3074(4)	0.020(1)
O9	O	0.8755(8)	¾	0.4366(4)	0.016(1)
O10	O	0.5610(7)	¼	0.1619(4)	0.012(1)
O11	O	0.3986(6)	¾	0.2476(4)	0.009(1)
O12	O	0.5389(7)	¾	0.1462(4)	0.013(1)
O13	O	0.2652(5)	0.4880(7)	0.1087(3)	0.0150(9)
O14	O	0.7921(5)	−0.0270(7)	0.1308(3)	0.0165(9)
O15	$O_{0.5}$	0.5527(9)	0.6768(9)	0.0046(5)	0.012(2)
O16	O	0.061(1)	¼	−0.0222(4)	0.036(2)
O17	O	0.0215(8)	¼	0.1171(4)	0.024(2)

occupied by Ca (A1) and REE (A2, A3 and A4). Three independent octahedral sites are present in the structure: M1 octahedra form branched chains with M3 octahedra alternately attached on opposite sides, whereas M2 octahedra form single chains. As in the case of the other members of the supergroup (Bonazzi *et al.*, 2017), the structure of these crystals can be described as a regular alternation of (0 0 1) epidote-type slabs (E) and (-102) törnebohmite-type slabs (T) (Fig. 6).

Ferriperbøeite-(Ce) is topologically identical to gatelite-(Ce) (Bonazzi *et al.*, 2003) and the other members of the supergroup. However, like in västmanlandite-(Ce), perbøeite-(Ce) and alnaperbøeite-(Ce), the split of the O15 oxygen atom, which slightly deviates from the mirror plane normal to the **b**-axis, indicates that the $P2_1/m$ structure ($a = ½\ a_{gat}$) is actually an average structure.

7.2. Cation distribution

Due to the fact that the main cation substitutions occur in the E module, the ionic species were assigned to the structural sites following the rules approved for epidote supergroup minerals (Armbruster *et al.*, 2006). The sum Si + P reproduces the stoichiometric constrains ($T = 5$) within a relative error of 1.4%, but the possible incorporation of minor Al at the tetrahedral sites was not considered and therefore all Al was assigned to the octahedral sites.

Analogously, the very low excess (4.02–4) of the octahedral cations (*i.e.* Fe^{2+}, Mg, Al, Fe^{3+}, Ti^{4+}) was considered to be reasonably within the experimental error and the A-sites were filled with Ca, Y and REE only; in particular, all Ca was assigned to A1 and the deficit (1–Ca) was compensated by the trivalent REE, while the A2, A3 and A4 sites were filled by REE. The overall mean electron number at the A sites obtained from the structure refinement (195.8 e^-) is in excellent agreement with that obtained with microprobe data (196.6 e^-).

As concerns the octahedral sites, all Al was assigned to the M2 sites and the deficit (2–Al) was compensated by Fe^{3+}. The remaining octahedral cations were then distributed between M3 and M1 taking into consideration the crystal-chemical requirements and the structural information obtained from the X-ray data. In particular, Fe and Mg were assigned to the large octahedron M3 in the proportions required by the refined site scattering value (*i.e.*, 23.1 e^-). Then, the Fe^{3+}/Fe^{2+} proportion was estimated on the basis of pure ⟨M3–O⟩ distances derived from known inter-atomic distances for members of the epidote supergroup [*i.e.* $\langle Fe^{3+}–O\rangle^{M3} = 2.055$ Å, $\langle Fe^{2+}–O\rangle^{M3} = 2.175$ Å (Bonazzi & Menchetti, 1995); ⟨Mg–O⟩ = 2.124 Å, extrapolated assuming a cation population of $0.87Mg + 0.13Fe^{2+}$ at M3 in dollaseite-(Ce) (Peacor & Dunn, 1988)]. The result requires that all Fe^{2+} is ordered at M3.

Table 5. Bond distances (in Å) in the structure of ferriperbøeite-(Ce).

A1–O7	2.320(6)	M2–O3	1.899(4)
A1–O3 (×2)	2.361(4)	M2–O10	1.902(4)
A1–O1 (×2)	2.389(4)	M2–O11	1.903(4)
A1–O5	2.496(6)	M2–O13	1.911(5)
A1–O6	2.903(6)	M2–O6	1.933(4)
A1–O9 (×2)	3.101(2)	M2–O12	1.963(4)
⟨A1–O⟩	2.602	⟨M2–O⟩	1.919
A2–O7	2.385(6)	M3–O8	1.946(6)
A2–O14 (×2)	2.451(4)	M3–O4	1.994(6)
A2–O10	2.654(6)	M3–O2 (×2)	2.161(4)
A2–O2 (×2)	2.660(4)	M3–O1 (×2)	2.242(4)
A2–O3 (×2)	2.755(4)	⟨M3–O⟩	2.124
⟨A2–O⟩	2.596		
		Si1–O7	1.579(6)
A3–O17	2.407(7)	Si1–O9	1.645(6)
A3–O14 (×2)	2.531(5)	Si1–O1 (×2)	1.644(4)
A3–O15 (×2)	2.534(8)	⟨Si1–O⟩	1.628
A3–O13 (×2)	2.546(4)		
A3–O12	2.763(6)	Si2–O8	1.590(6)
A3–O15 (×2)	2.933(8)	Si2–O9	1.621(6)
⟨A3–O⟩	2.626	Si2–O3 (×2)	1.624(4)
		⟨Si2–O⟩	1.615
A4–O16	2.259(6)		
A4–O2 (×2)	2.525(4)	Si3–O2 (×2)	1.623(4)
A4–O11	2.597(5)	Si3–O6	1.650(6)
A4–O14 (×2)	2.659(4)	Si3–O5	1.662(6)
A4–O13 (×2)	2.753(4)	⟨Si3–O⟩	1.640
A4–O17 (×2)	2.965(2)		
⟨A4–O⟩	2.666	Si4–O14 (×2)	1.616(4)
		Si4–O15	1.629(8)
M1–O4 (×2)	1.918(4)	Si4–O12	1.645(6)
M1–O5 (×2)	2.029(4)	⟨Si4–O⟩	1.627
M1–O1 (×2)	2.040(4)		
⟨M1–O⟩	1.996	Si5–O16	1.572(7)
		Si5–O17	1.614(7)
		Si5–O13 (×2)	1.635(4)
		⟨Si5–O⟩	1.614

Table 6. Experimental X-ray powder diffraction data (*d* in Å) for ferriperbøeite-(Ce).

I	d_{obs}	d_{calc}	*h*	*k*	*l*
13	15.88	15.8289	0	0	1
7	8.03	8.0254	$\bar{1}$	0	0
4	4.83	4.8272	$\bar{1}$	1	1
14	4.71	4.6978	1	0	2
22	4.67	4.6709	$\bar{1}$	1	0
6	4.39	4.3961	$\bar{1}$	0	4
10	4.20	4.1983	1	1	1
8	3.951	3.9572	0	0	4
7	3.875	3.8858	0	1	3
45	3.520	3.5193	$\bar{2}$	1	2
20	3.488	3.4910	$\bar{1}$	1	4
9	3.394	3.3928	2	1	3
11	3.285	3.2895	2	1	0
16	3.123	3.1237	1	1	3
18	3.080	3.0757	$\bar{2}$	0	2
100	2.997	3.0007	$\bar{1}$	1	5
45	2.868	2.8720	0	2	0
40	2.771	2.7726	0	1	5
25	2.703	2.7041	1	2	0
34	2.682	2.6775	$\bar{2}$	0	3
60	2.633	2.6302	$\bar{3}$	1	2
6	2.522	2.5225	0	2	3
12	2.453	2.4531	$\bar{3}$	1	5
10	2.292	2.2930	$\bar{3}$	0	7
16	2.282	2.2827	$\bar{2}$	2	4
7	2.260	2.2613	0	0	7
23	2.190	2.1869	$\bar{4}$	0	2
27	2.159	2.1616	$\bar{2}$	2	5
14	2.125	2.1271	0	2	5
35	2.100	2.0991	2	2	2
10	2.092	2.0967	3	1	2
12	2.082	2.0807	$\bar{2}$	0	5
10	2.062	2.0642	$\bar{3}$	2	3
6	1.995	1.9980	$\bar{4}$	0	7
4	1.976	1.9786	0	0	8
22	1.959	1.9625	$\bar{3}$	1	8
16	1.954	1.9585	2	2	3
13	1.933	1.9311	$\bar{3}$	1	3
11	1.900	1.8826	$\bar{2}$	2	7
17	1.859	1.8577	1	1	7

The ⟨M1–O⟩ distance is smaller than the corresponding value (2.007 Å) found in västmanlandite-(Ce) where the site M1 is occupied by $0.81Mg + 0.19Fe^{3+}$ (Holtstam *et al.*, 2005). The ⟨M2–O⟩ distance is slightly greater than that observed for the fully Al-occupied M2 in perbøeite-(Ce) (Bonazzi *et al.*, 2014).

Although the hydrogen atoms were not located on the difference Fourier map, two short O–O contacts (*i.e.* O10–O15 = 2.673 and O11–O4 = 2.969 Å), which do not define polyhedral edges, compare well with the corresponding values found in the alnaperbøeite-(Ce)–perbøeite-(Ce) members (2.642–2.689 and 2.939–2.990 Å for O10–O15 and O11–O4, respectively) and involve hydrogen bonding with O10 and O11 as donor O atoms. The hydrogen-bonding system in ferriperbøeite-(Ce) is confirmed by the empirical bond-valence sums (calculated on the basis of the bond parameters given by Brese & O'Keeffe, 1991) on O10 and O11 oxygen donors (1.27 and 1.29 *v.u.*, respectively), and on O15 and O4 oxygen acceptors (1.55 and 1.59 *v.u.*, respectively). From the empirical correlation function of O…O distances versus the frequency of O–H stretching modes established by Libowitzky (1999), OH bands in ferriperbøeite-(Ce) are expected at *ca.* 3540 and 3100 cm^{-1}. The two relatively sharp bands observed at 3590 and 3520 cm^{-1} (Fig. 3) match the prediction for the O11–O4 contact very well. The two (or more) broad bands in the region 3300–3200 cm^{-1} are tentatively attributed to the O–H stretching in O10–H…O15. It can be noted that for perbøeite-(Ce), Chukanov & Chervonnyi (2016) report two broad bands at 3270 and 3180 cm^{-1}, respectively.

The resulting overall crystal-chemical formula is: $^{A1}[\mathbf{Ca_{0.92}}REE_{0.08}]$ $^{A2,A3,A4}[\mathbf{REE_3}]$ $^{M1}[\mathbf{Fe^{3+}_{0.65}}Mg_{0.35}]$ $^{M2}[Al_{1.85}\ Fe^{3+}_{0.15}]$ $^{M3}[\mathbf{Fe^{2+}_{0.46}}\ Fe^{3+}_{0.33}Mg_{0.21}][Si_2O_7][SiO_4]_3\mathbf{O}(OH)_2$, where the dominant, species-defining atoms are written in bold.

The fitted Mössbauer spectrum is shown in Fig. 4. The sub-spectra A and C due to Fe^{3+} [isomer shift = 0.35(1) and 0.37(1)] are interpreted to belong to M3 + M1 (A) and M2 (C), respectively (Table 7). Their absorption area sums

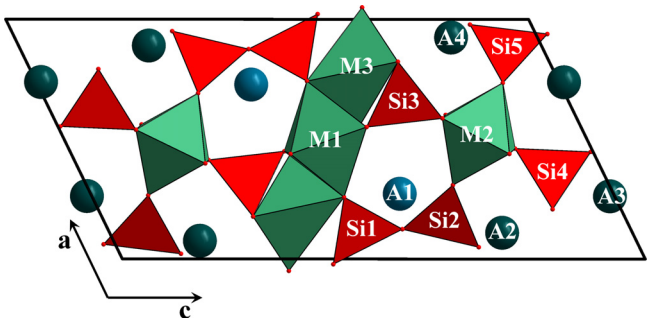

Fig. 5. Unit-cell content of ferriperbøeite-(Ce) down [0 1 0]. Circles represent A atoms, whereas M and Si atoms are depicted as polyhedra. The unit cell and the orientation of the structure are outlined.

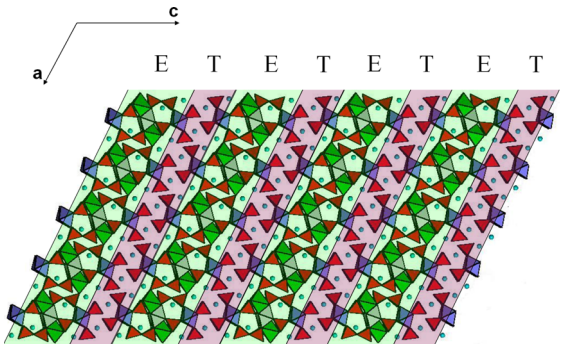

Fig. 6. Crystal structure of ferriperbøeite-(Ce) seen as a regular alternation of (0 0 1) epidote-type slabs (E) and ($\bar{1}$ 0 2) törnebohmite-type slabs (T). **E** = A1 A2 M1 M2 M3[$(Si_2O_7)(SiO_4)$]O(OH) ; **T** = A3 A4 M2$[SiO_4]_2$(OH).

Table 7. Hyperfine Mössbauer parameters for ferriperbøeite-(Ce).

Sub-spectrum	Isomer shift (mm/s)	Quadrupole splitting (mm/s)	Absorption area (%)	FWHM (mm/s)	Assignment
A	0.35(1)	1.86(1)	46(1)	0.34(1)	Fe^{3+} in M1 + M3
B	1.08(1)	1.76(1)	31(1)	0.38(1)	Fe^{2+} in M3
C	0.37(1)	0.73(3)	23(3)	0.69(7)	Fe^{3+} in M2

to 69% of total Fe, which compares favourably with the value estimated from single-crystal data (71%). The sub-spectrum B represents Fe^{2+} at a single, highly distorted octahedral site and is interpreted as Fe^{2+} at M3 [isomer shift = 1.08 (1)]. The overall Fe^{2+}/Fe^{3+} ratio obtained by Mössbauer spectroscopy (0.45) is in excellent accord with that obtained from the structural analysis (0.41).

From the structural data, however, we expect a small fraction (below 10%) of Fe^{3+} to reside at M2, but from the Mössbauer data a higher value, 23%, is obtained (Table 7). This could at least in part be related to the fact that the corresponding absorption peak is less well resolved than the others; which leads to a significantly broader line width. If the FWHM value is constrained to a fixed value of 0.40 mm/s in the spectrum fitting procedure, the absorption area of the C sub-spectrum is reduced to 16.2(5)%, with little change of the other parameters. Nevertheless, because contamination by ferriallanite-(Ce) in the sample cannot be excluded, the spectroscopic evidence of a high content of Fe^{3+} at a regular octahedral site (M2) could be due to the contribution of Fe^{3+} hosted at the M2 site of ferriallanite-(Ce): in such a mineral from Nya Bastnäs studied by Holtstam *et al.* (2003), however, the M2 site was found to contain only 6 ± 2% of the total Fe content (corresponding to *ca.* 0.12 Fe^{3+} pfu). Törnebohmite-(Ce) from Nya Bastnäs has been found to contain up to maximum 1.9% Fe_2O_3 (*ca.* 0.12 Fe^{3+} pfu; Holtstam & Andersson, 2007) and might as well have contributed to the observed absorption, but only to a small extent.

7.3. Formation of the mineral

The inferred paragenetical sequence from textural observations is cerite-(Ce) → ferriperbøeite-(Ce) + törnebohmite-(Ce) → ferriallanite-(Ce) → bastnäsite-(Ce) → sulphides. As it has been found as the general rule for ferriallanite-(Ce) in the subtype-1 deposits (Geijer, 1921; Holtstam & Andersson, 2007), ferriperbøeite-(Ce) in this specimen has largely formed from metasomatic alteration of cerite-(Ce). A hydrothermal fluid which has already been deprived of most of its REE content, but with significant Al, Fe and Si in aqueous solution, reacts with cerite-(Ce) according to:

$$5Al^{3+}(aq) + Fe^{2+}/2Fe^{3+}(aq) + 5(SiO_4)^{4-}(aq) + H_2O + \underset{\text{cerite}-(Ce)}{(Ce_8Ca_2)Mg[SiO_4]_3[SiO_3OH]_4(OH)_3} \rightarrow \underset{\text{ferriperbøeite}-(Ce)}{2[CaCe_3][Fe^{3+}Al_2Fe^{2+}_{0.5}Mg_{0.5}][Si_2O_7][SiO_4]_3O(OH)_2} + \underset{\text{törnebohmite}-(Ce)}{Ce_2Al(SiO_4)_2(OH)} + 4H^+$$

For simplicity, the speciation of Al and Fe is not given above, but presumably, various hydroxide-fluoride and chloride species are dominant. The reaction explains the ubiquitous presence of törnebohmite-(Ce) in the assemblage. From the molar volumes of the solid products, it is calculated that *ca.* 17% by volume is törnebohmite-(Ce), in good agreement with the petrographic observations.

Acknowledgments: The authors are really glad to contribute to this issue dedicated to Giovanni Ferraris and Stefano Merlino, two of the most prominent figures in mineralogical crystallography. Their long-standing studies on mineral crystal-chemistry in general, and on modular aspects in particular, are especially noteworthy, and they undoubtedly represent a solid basis for the next generations. Giovanni and Stefano perfectly symbolize the ideal bridge between mineralogy and the most advanced fields of crystallography.

LB and PB thanks the University of Florence, "Progetto di Ateneo 2015". DH acknowledges a previous grant to study the Bastnäs-type deposits, from the Swedish Research Council (contract #2003-3572). Thanks are due to Henrik Skogby, Swedish Museum of Natural History, who assisted with FTIR measurements. The paper benefited by the official reviews made by Taras L. Panikorovskii and an anonymous reviewer.

References

Armbruster, T., Bonazzi, P., Akasaka, M., Bermanec, V., Chopin, C., Gieré, R., Heuss-Assbichler, S., Liebscher, A., Menchetti, S., Pan, Y., Pasero M. (2006): Recommended nomenclature of epidote-group minerals. *Eur. J. Mineral.*, **18**, 551–567.

Bonazzi, P. & Menchetti, S. (1995): Monoclinic members of the epidote group: effects of the $Al \leftrightarrow Fe^{3+} \leftrightarrow Fe^{2+}$ substitution and of the entry of REE^{3+}. *Mineral. Petrol.*, **53**, 133–153.

Bonazzi, P., Bindi, L., Parodi, G. (2003): Gatelite-(Ce), a new REE-bearing mineral from Trimouns, French Pyrenees: crystal structure and polysomatic relationships with epidote and törnebohmite-(Ce). *Am. Mineral.*, **88**, 223–228.

Bonazzi, P., Lepore, G.O., Bindi, L., Chopin, C., Husdal, T., Medenbach, O. (2014): Perbøeite-(Ce) and alnaperbøeite-(Ce), two new members of the epidote-törnebohmite polysomatic series: Chemistry, structure, dehydrogenation, and clue for a sodian epidote end-member. *Am. Mineral.*, **99**, 157–169.

Bonazzi, P., Holtstam, D., Bindi, L. (2017): A proposal to establish groups within a gatelite supergroup, and recommended nomenclature. Memorandum 80_SM75, approved by IMA-CNMNC.

Brese, N.E. & O'Keeffe, M. (1991): Bond-valence parameters for solids. *Acta Crystallogr.*, **B47**, 192–197.

Chukanov, N.V. & Chervonnyi, A.D. (2016): Infrared spectroscopy of minerals and related compounds. Springer, 1109 p.

Geijer, P (1921): The cerium minerals of Bastnäs at Riddarhyttan. *Sver. Geol. Unders. Avh.*, **C304**, 1–24.

Gurzhiy, V.V., Karimova, O.V., Kartashov, P.M., Krivovichev, S.V., (2010): Crystal structure of a new member of the polysomatic series törnebohmite-epidote from carbonatites of Eastern Siberia. International Mineralogical Association Meeting Budapest, August 2010, Abstract Volume, 744 p.

Holtstam, D. & Andersson, U.B. (2007): The REE minerals of the Bastnäs-type deposits, South-Central Sweden. *Can. Mineral.*, **45**, 1073–1114.

Holtstam, D., Andersson, U., Mansfeld, J. (2003): Ferriallanite-(Ce) from the Bastnäs deposit, Västmanland, Sweden. *Can. Mineral.*, **41**, 1233–1240.

Holtstam, D., Kolitsch, U., Andersson, U.B. (2005): Västmanlandite-(Ce) – a new lanthanide- and F-bearing sorosilicate mineral from Västmanland, Sweden: description, crystal structure, and relation to gatelite-(Ce). *Eur. J. Mineral.*, **17**, 129–141.

Holtstam, D., Andersson, U.B., Broman C., Mansfeld, J. (2014): Origin of REE mineralization in the Bastnäs-type Fe-REE-(Cu-Mo-Bi-Au) deposits, Bergslagen, Sweden. *Mineral. Dep.*, **49**, 933–966.

Jonsson, E. & Högdahl, K. (2013): New evidence for the timing of formation of Bastnäs-type REE mineralisation, Bergslagen, Sweden. *in* "12th SGA Biennial Meeting, Proc.", Volume **4**, 1724–1727.

Kartashov, P., Ferraris, G., Ivaldi, G., Sokolova, E., McCammon, C. A. (2002): Ferriallanite-(Ce), $CaCeFe^{3+}AlFe^{2+}(SiO_4)(Si_2O_7)O(OH)$, a new member of the epidote group: description, X-ray and Mössbauer study. *Can. Mineral*, **40**, 1641–1648.

Libowitzky, E. (1999): Correlation of O–H stretching frequencies and O–H…O hydrogen bond lengths in minerals. *Monatsh. Chem.*, **130**, 1047–1059.

Mandarino, J.A. (1981): The Gladstone-Dale relationship. IV. The compatibility concept and its application. *Can. Mineral.*, **19**, 441–450.

Oxford Diffraction (2006): *CrysAlis* RED (Version 1.171.31.2) and ABSPACK in *CrysAlis* RED. Oxford Diffraction Ltd, Abingdon, Oxfordshire, England.

Peacor, D.R. & Dunn, P.J. (1988): Dollaseite-(Ce) (magnesium orthite redefined): structure refinement and implications for $F + M^{2+}$ substitutions in epidote-group minerals. *Am. Mineral.*, **73**, 838–842.

Prescher, C., McCammon, C., Dubrovinsky, L. (2012): *MossA*: a program for analyzing energy-domain Mössbauer spectra from conventional and synchrotron sources. *J. Appl. Crystallogr.*, **45**, 329–331.

Sheldrick, G.M. (2013): SHELXL2013. University of Göttingen, Germany.

Smith, D.G.W. & Nickel, E.H. (2007): A system of codification for unnamed minerals: report of the Subcommittee for Unnamed Minerals of the IMA Commission on New Minerals, Nomenclature and Classification. *Can. Mineral.*, **45**, 983–1055.

Wilson, A.J.C., ed. (1992): International Tables for Crystallography, Volume C: mathematical, physical and chemical tables. Kluwer Academic, Dordrecht, NL.

Ya'acoby, A. (2011): The petrology and petrogenesis of the Ren carbonatite sill and fenites, southeastern British Columbia, Canada. MSc thesis, University of British Columbia, 463 p.

Received 7 August 2017
Modified version received 20 September 2017
Accepted 30 September 2017